




# New Real-Time Sub-Terahertz Security Body Scanner

Gombo Tzydynzhapov<sup>1,2</sup> · Pavel Gusikhin<sup>1,2</sup>  · Viacheslav Muravev<sup>1,2</sup> · Alexey Dremin<sup>1,2</sup> · Yuri Nefyodov<sup>1,2</sup> · Igor Kukushkin<sup>1,2</sup>

Received: 13 August 2019 / Accepted: 20 February 2020 / Published online: 07 March 2020  
© Springer Science+Business Media, LLC, part of Springer Nature 2020

## Abstract

In response to the urgent demand for efficient, safe, and speedy imaging in remote security screening applications, a new sub-terahertz security body scanner has been developed. Integration of innovative THz sensing technique and advanced IMPATT-diode-based signal-generating technology resulted in a cost-effective cutting-edge system capable of real-time visualization of the threats hidden under the clothes of people. This paper introduces the new 100-GHz security scanner and presents the test results which demonstrate that it can perform through-garment detection at standoff ranges of 3–6 m with respective lateral resolution of 3–6 cm. The depth of the field of the system has been determined experimentally to be approximately 30 cm.

**Keywords** Terahertz (THz) · Terahertz imaging · Body scanner · Security · Real-time · Remote imaging

## 1 Introduction

In light of modern technological advancements, terahertz and sub-terahertz radiation has been increasingly gaining in popularity as safe and effective means of nondestructive testing (NDT) for internal anomalies and defects [1, 2]. Research into detection of chemical changes in biological systems using terahertz spectroscopy [3–5] is also underway. In addition, sub-THz imaging instrumentation provides for efficient detection and identification of concealed objects of life-threatening nature, such as weapons or explosives, in security screening [6, 7]. As THz radiation at moderate power levels poses no health risk to the human body [8] and since in this frequency spectrum most common clothing becomes essentially transparent [9], modern THz scanning systems have advantages over the conventional equipment. The most

---

✉ Pavel Gusikhin  
[gusikhin@issp.ac.ru](mailto:gusikhin@issp.ac.ru)

<sup>1</sup> Institute of Solid State Physics RAS, Chernogolovka, 142432, Russia

<sup>2</sup> Terasense Group, Inc., San Jose, CA, 95110, USA

promising of which is the possibility to detect and differentiate between objects made of various materials. Moreover, compared with standard commercial technology, such as X-ray imagers and portal-based screening schemes, which are bulky and stationary structures operated in close proximity to the target, compact and portable THz imaging systems are capable of detecting concealed threats remotely. Therefore, such kind of a system can be easily hidden or camouflaged to enable clandestine security surveillance.

As of today, commercially available microwave security screening systems operate at fairly low frequencies. Thus, they work in the near field and have rather poor lateral resolution due to physical restrictions. Consequently, there have been proposed a number of imaging techniques in sub-THz and THz frequency ranges in order to overcome these limitations [10], including imaging radar technique [11–15], near-field imaging [16], and imaging by multistatic array [17, 18]. Although these systems offer substantial sensitivity and good resolution at a considerable detection range, currently their performance is hindered significantly by low imaging speed, with typical frame rates of around 1 fps. Hence, in a real-life scenario, this limitation may seriously interfere with smooth passenger traffic moving through a security checkpoint.

As a more effective alternative to existent active radar imaging technology, we have devised a new sub-THz security body scanner for the remote screening with comparable sensitivity and resolution, yet with far superior image frame rate. Unlike the radar approach, in this system, an object hidden on the human body is imaged based on measured power intensity distribution of the radiation reflected from the target. Similar operating mode has been employed in imagers with focal-plane arrays developed on the basis of microbolometers, silicon CMOS circuits, pyroelectric devices, and high-electron-mobility transistors (HEMTs) [19–22]. Although these commercially available detector arrays permit video-rate imaging at room temperature, they are significantly restricted in their overall size, as determined by pixel dimensions and the number of pixels. In our case, livestream imaging speed has been achieved owing to novel-type terahertz semiconductor detectors capable of ultra-fast operation at room temperature [23, 24].

In this paper, we introduce the new terahertz security body scanner. We describe its key components, give an overview of its distinctive technical features, and summarize the test results to demonstrate its performance in detection of person-borne concealed objects. We also remark on some current limitations of the system and consider its prospective improvement.

## 2 System Description

The new sub-terahertz security body scanner is a complete imaging system that incorporates terahertz instrumentation produced by TeraSense (Fig. 1). It includes six IMPATT-diode sources radiating at a fixed frequency with the exact operating frequency varying slightly between the sources from 96 to 98 GHz with linewidth  $\sim 1$  MHz. The output power of each source is approximately 80 mW. Frequency and linewidth were measured by the Agilent E4407B spectrum analyzer with



**Fig. 1** Photograph of the new terahertz security body scanner. On the left, complete system setup—fixed geometrical arrangement of six 100-GHz sources with imaging camera at the center. Displayed on the right are enlarged photos of a single generator (at the top) and a camera assembly (at the bottom), to illustrate the details of adjustable mechanical fixtures and positions of the condenser lens and the objective lens, respectively

Agilent 11970W harmonic mixer. Output power was measured by the VDI Erickson PM5 power meter. Each source is equipped with a protective isolator, high-gain conical horn antenna, and aspherical collimating PTFE lens.

The primary feature of the body scanner is its real-time imaging camera, which relies on a new method of plasmonic detection [23, 24] that makes possible ultra-fast sensing of THz radiation at room temperature. The camera has  $32 \times 32$  array of pixels with size of  $3 \times 3$  mm, effective responsivity of  $50 \pm 10$  kV/W at 96–98 GHz, and noise equivalent power of  $1 \text{ nW/Hz}^{1/2}$ . Image is formed by the aspherical PTFE objective lens with focal length of 386 mm and aperture of 300 mm.

The security screening system is designed to function in reflection mode, as illustrated in Fig. 2, when the area of interest is irradiated with the sources and the reflected radiation is collected by the objective lens and imaged by the camera. Since in the given frequency spectrum reflection from most objects is specular, multiple sources are required to provide maximum illumination of the area of interest at different angles for enhanced image quality. In the given configuration, the scanner is capable of revealing hidden objects at a standoff distance of 3–6 m from objective lens. The position and orientation of each generator and its collimating lens are adjusted to ensure that incident radiation from all six sources converges in the area of interest at a specified range.

The overall system is controlled by the TeraSense Viewer software available in C++ SDK or LabView SDK. It is a user-friendly interface that allows for prompt signal acquisition, image visualization, and basic data processing including background compensation and image smoothing.

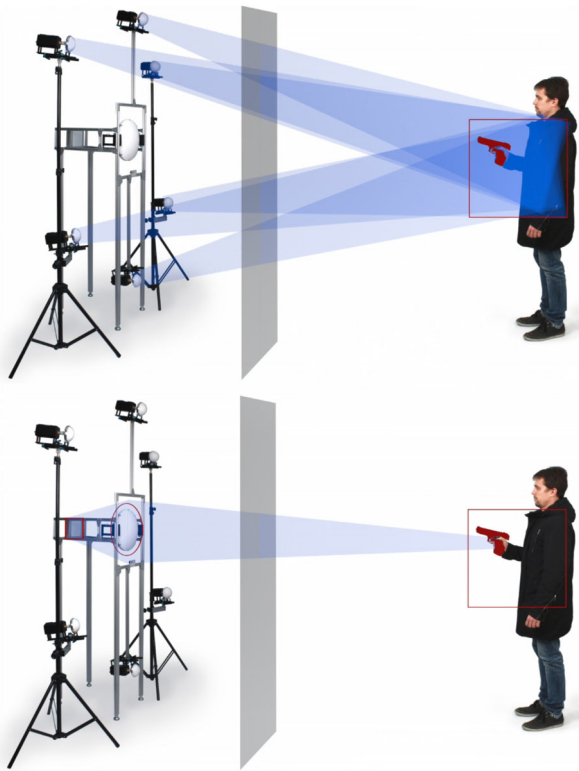


**Fig. 2** Illustration of the scanner operation in reflection mode at a 3-m standoff range. Both the system and the man are shown to scale. At the top—the area of interest is maximally illuminated with sub-THz radiation at different angles. At the bottom—the reflected radiation is collected by the objective lens and projected onto the imaging camera

### 3 Measurement Results

We conducted several tests to evaluate the performance of the new security scanner. Firstly, we measured the radiation pattern of the transmitting conical horn antenna to determine the actual beam profile of the irradiance generated by the IMPATT-diode source. The measurements were conducted by the mechanical scanning of single calibrated  $1.5 \times 1.5$  mm detector in plane perpendicular to the optical axis on the distance of 25 cm from the horn antenna output.

The beam patterns displayed in Fig. 3 demonstrate that both *E*-plane and *H*-plane profiles are in good agreement with theoretical curves computed for the given horn antenna dimensions, 12-mm aperture diameter and 40-mm length.

The test data also indicate the beam divergence of  $18^\circ$ , which translates into an illuminated area of 1 m in diameter at a 3-m range from the source. Since at this distance the given optical system provides  $60 \times 60$  cm field of view, we introduced an additional condenser lens to further focus the source beam. For this purpose, we

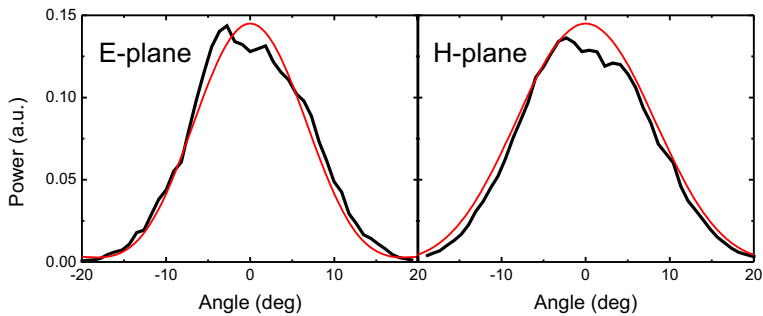


**Fig. 3** *E*-plane and *H*-plane radiation pattern of the horn antenna used with IMPATT-diode source. The measured and calculated data are plotted with black and red lines, respectively

used PTFE plano-convex aspherical lens with clear aperture of  $D = 90$  mm and focal length of  $f = 50$  mm.

Adjusting the position of the collimating lens relative to the source allows for reduction in the beam divergence to match the desired field of view. Figure 4 shows the lateral distribution of irradiated power obtained for different separation between the lens and the antenna at the distance of 25 cm from the lens. The separation of 45 mm corresponds to the minimal beam divergence limited by the diffraction limit:  $\theta_{\min} = 1.22\lambda/D \approx 2.3^\circ$ . Figure 5 shows the lateral distribution of irradiated power obtained for separation between the lens and the antenna of 45 mm at different distances from the lens.

Secondly, we assessed the focusing capability of the quasi-optical system consisting of a sub-THz imaging camera and a PTFE objective lens. Figure 6 shows data obtained from the lateral resolution test, where two small circular targets (foil balls) are imaged at a 3-m range with progressively decreasing offset between them. The measurements evidence that spatial resolution of the scanner at this standoff distance

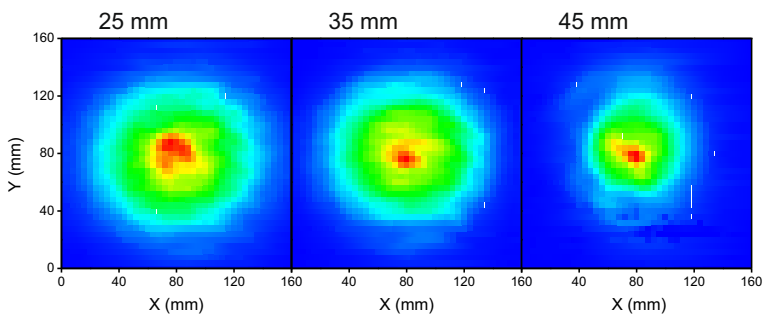


**Fig. 4** Distribution of irradiated power measured at the distance of 25 cm from the collimating lens. Distance between the output of the horn antenna and the collimating lens was 25, 35, and 45 mm (from the left to the right)

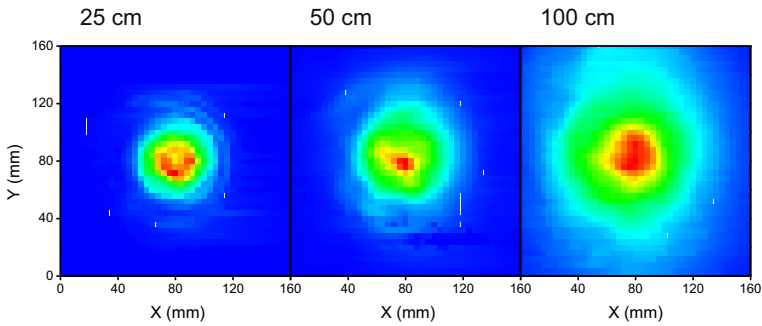


**Fig. 5** From left to right: distribution of irradiated power measured at the distances of 25, 50, and 100 cm from the source with a condenser lens

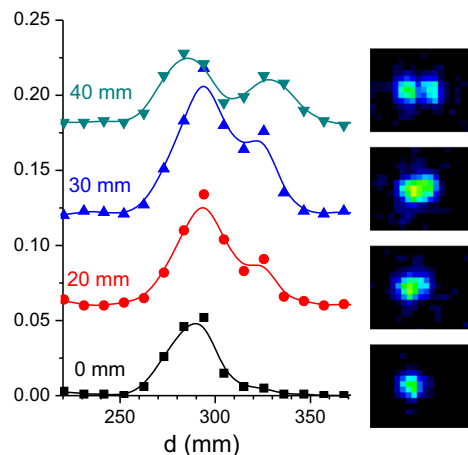
approaches 3 cm. Analogous test at a greater range of 6 m resulted in resolution of 6 cm. Theoretical limit for the resolution of an optical system is determined by:

$$R = 1.22 \frac{\lambda}{D} a, \quad (1)$$

where  $a$  is a distance between object and objective lens. In our case, (1) gives  $R = 3.7$  cm for  $a = 3$  m and  $R = 7.3$  cm for  $a = 6$  m. So, the performance of our system is limited only by the diffraction limit.

We conducted measurements to determine depth of the field of the system based on detection of two closely spaced targets, at the distance varying around 3 m away from the system. The measurement results presented in Fig. 7 indicate that given camera aperture size allows for nearly 30-cm depth of field, where the two targets are still discriminated within the incremental range displacement interval from  $-20$  to  $+10$  cm. From the practical standpoint, both parameters, the target imaging area and the depth of field, are found to be suitable for sensing person-borne concealed threats.

**Fig. 6** System resolution test results. Two circular targets, 30 mm in diameter are imaged at a 3-m standoff range. Each trace with corresponding image on the right represents the response of the target doublet measured at the indicated target separation,  $d$ . The traces are offset for clarity of illustration



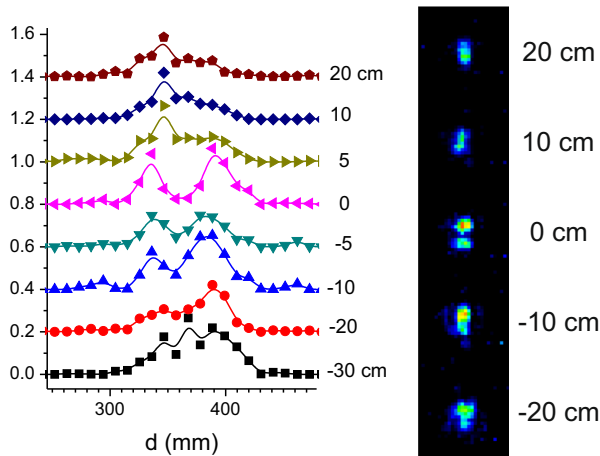


**Fig. 7** Measurement results for the depth of field. Two targets, 30 mm in diameter, are offset by  $d = 60$  mm and are initially placed 3 m away from the camera. Graphs and corresponding images represent target response measured at indicated displacements in range

In order to characterize the image quality across the field, we took a set of measurements at a separation distance of 3 m with a single source projecting radiation beam towards the camera from different points within the full planar field of view of the camera and at different incident angles. From the data displayed in Fig. 8 it is evident that physical limitations of the objective lens cause only slight deterioration in image quality occurring around the periphery, i.e., image sharpness across the field of view remains sufficiently uniform to serve the application purpose.

Finally, Fig. 9 illustrates real-life sub-terahertz visualization of the threats covered by typical clothing that we accomplished with the new security body scanner. As shown in the figure, the contrast images obtained at a 3-m standoff range are adequate for target detection and general classification since they clearly convey the

**Fig. 8** Imaging results demonstrating the focusing capability of the camera and the objective lens across the entire field of view of the system. The measurements are taken with a single source pointed at the camera from 3-m distance. The source is displaced vertically and horizontally in 10-cm increments

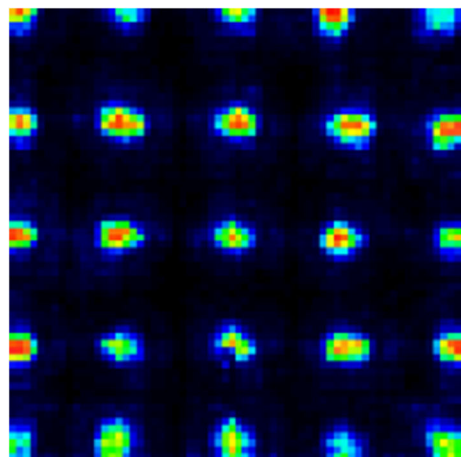




**Fig. 9** Imaging results of a real-life visualization of body-borne concealed threats, a belt with explosives and a gun, obtained by the new sub-THz security body scanner at 3-m range

proportions, the relative size, the shape, and the spatial orientation of each hidden object. The figure also demonstrates a special system software feature of creating an overlay picture of the actual sub-terahertz target image and the corresponding visible range image of a person to ease prompt visual interpretation.

## 4 Conclusion

We have introduced the new 100-GHz security body scanner. We have given an overview of its essential innovative components that enable remote sub-THz sensing of body-borne concealed threats at livestream imaging speed, which is the key competitive feature of the system. Experimental results confirm that other performance parameters of the scanner, such as imaging area, depth of field, and lateral resolution, also meet the typical application requirements. The ultimate real-life test has proven the system capable of through-garment detection of a simulated belt with explosives or a gun at a 3-m range, which is a sufficient standoff distance for deploying the system to perform remote covert screening at conventional security check points.

However, the apparatus still has a few limitations, one of which is its moderate spatial resolution of 3–6 cm. Since it is directly dependent on the operating frequency, upgrading the system by increasing frequency would provide for threefold improvement in resolution.

Another factor that presently inhibits image quality is that due to specular target reflection in the given frequency spectrum, considerable amount of produced glare



escapes the objective lens. Therefore, we are working on development of a more efficient target illumination scheme in order to increase the effective aperture of the camera.

One more physical constraint of the current system configuration is its restriction to 2D imaging. Since at given wavelengths, the human body itself reflects most of the incident radiation, in some cases, distinguishing a target from such background clutter with sufficient contrast becomes rather challenging. Hence, more work is being done towards implementation of additional depth resolution.

All things considered, the new security body scanner is a powerful and cost-effective solution that has a potential to meet the urgent demand for fast and reliable remote security screening for concealed threats.

**Acknowledgments** The authors would like to recognize Dr. Oleg Khrichenko, a technical writing specialist at Terasense Group Inc., for his substantial contribution to drafting, language editing, and proofreading of the manuscript.

**Funding Information** The authors gratefully acknowledge the financial support from the Russian Science Foundation (Grant No. 19-72-30003).

## References

1. H. Zhong, J. Xu, X. Xie, T. Yuan, R. Reightler, E. Madaras, and X.-Ch. Zhang, Nondestructive defect identification with terahertz time-of-flight tomography, *IEEE Sensors Journal*, vol. 5, no. 2, pp. 203–208 (2005).
2. I. Amenabar, F. Lopez, and A. Mendikute, In introductory review to THz non-destructive testing of composite mater, *Journal of Infrared, Millimeter, and Terahertz Waves*, vol. 34, issue 2, pp. 152–169 (2013).
3. D. F. Plusquellic, K. Siegrist, E. J. Heilweil, and O. Esenturk, Applications of terahertz spectroscopy in biosystems, *Chem. Phys. Chem.*, vol. 8, pp. 2412–2431 (2007).
4. A. G. Markelz, Terahertz dielectric sensitivity to biomolecular structure and function, *IEEE J. Sel. Top. Quant.*, vol. 14, no. 1, pp. 180–190 (2008).
5. H. Cheon, H. Yang, S.-H. Lee, Y. A. Kim, and J.-H. Son, Terahertz molecular resonance of cancer DNA, *Sci. Rep.*, vol. 6, 37103 (2016).
6. K. Kawase, Y. Ogawa, Y. Watanabe, and H. Inoue, Non-destructive terahertz imaging of illicit drugs using spectral fingerprints, *Opt. Express*, vol. 11, issue 20, pp. 2549–2554 (2003).
7. Y. C. Shen, T. Lo, P. F. Taday, B. E. Cole, W. R. Tribe, and M. C. Kemp, Detection and identification of explosives using terahertz pulsed spectroscopic imaging, *Appl. Phys. Lett.* vol. 86, 241116 (2005).
8. *IEEE Standard for Safety Levels With Respect to Human Exposure to Radio Frequency Electromagnetic Fields*, 3 kHz to 300 GHz, IEEE Int. Committee on Electromagnetic Safety C95.1 (2005).
9. D. M. Sheen, D. L. McMakin, and T. E. Hall, Three-dimensional millimeter-wave imaging for concealed weapon detection, *IEEE Trans. on Microw. Theory and Techn.*, vol. 49, pp. 1581–1591 (2001).
10. P. Hillger, J. Grzyb, R. Jain, and U. R. Pfeiffer, Terahertz Imaging and Sensing Applications With Silicon-Based Technologies, in *IEEE Trans. on Terahertz Sci. and Technol.*, vol. 9, no. 1, pp. 1–19 (2019).
11. K. B. Cooper, R. J. Dengler, N. Llombart, T. Bryllert, G. Chattopadhyay, E. Schlecht, J. Gill, C. Lee, A. Skalare, I. Mehdi, and P. Siegel, Penetrating 3-D Imaging at 4- and 25-m Range Using a Submillimeter-Wave Radar, *IEEE Trans. on Microw. Theory and Techn.*, vol. 56, no. 12, pp. 2771–2778 (2008).

12. H. Essen, S. Stanko, R. Sommer, A. Wahlen, R. Brauns, J. Wilcke, W. Johannes, A. Tessmann, and M. Schlechtweg, A high performance 220-GHz broadband experimental radar, in *Proc. 33rd Int. Conf. Infrared, Millim., Terahertz Waves*, Pasadena, CA, USA (2008).
13. K. B. Cooper, R. J. Dengler, N. Llombart, B. Thomas, G. Chattopadhyay, and P. Siegel, THz Imaging Radar for Standoff Personnel Screening, *IEEE Trans. on Terahertz Sci. Technol.*, vol. 1, no. 1, pp. 169–182 (2011).
14. T. Jaeschke, C. Bredendiek and N. Pohl, A 240 GHz ultra-wideband FMCW radar system with on-chip antennas for high resolution radar imaging, *2013 IEEE MTT-S International Microwave Symposium Digest (MTT)*, Seattle, WA, pp. 1–4 (2013).
15. J. Grajal, A. Badolato, G. Rubio-Cidre, L. Úbeda-Medina, B. Mencia-Oliva, A. Garcia-Pino, B. Gonzalez-Valdes, and O. Rubiños, 3-D high-resolution imaging radar at 300 GHz with enhanced FoV, in *IEEE Trans. on Microw. Theory and Techn.*, vol. 63, no. 3, pp. 1097–1107 (2015).
16. Y. Zhao, X. Deng, B. Cheng, and J. Liu, 0.14THz imaging system for security and surveillance, in *Int. Conf. on Infrared, Milli. and Terahz Waves, IRMMW-THz* (2017).
17. S. S. Ahmed, A. Schiessl, and L. Schmidt, A novel fully electronic active real-time imager based on a planar multistatic sparse array, *IEEE Trans. on Microw. Theory and Techn.*, vol. 59, no. 12, pp. 3567–3576 (2011).
18. S. S. Ahmed, A. Genghammer, A. Schiessl, and L.-P. Schmidt, Fully electronic E-band personnel imager of 2 m<sup>2</sup> aperture based on a multistatic architecture, *IEEE Trans. on Microw. Theory and Techn.*, vol. 61, no. 1, pp. 651–657 (2013).
19. E. Hack, L. Valzania, G. Gaumann, M. Shalaby, C. Hauri, and P. Zolliker, Comparison of thermal detector arrays for off-axis THz holography and real-time THz imaging, *Sensors*, vol. 21, no. 2, p. 221 (2016).
20. U. Pfeiffer, and E. Ojefors, A 600-GHz CMOS focal-plane array for terahertz imaging applications, *ESSCIRC 2008 - 34th European Solid-State Circuits Conference*, Edinburgh, pp. 110–113 (2008).
21. E. Ojefors, N. Baktash, Y. Zhao, R. A. Hadi, H. Sherry, and U. R. Pfeiffer, Terahertz imaging detectors in a 65-nm CMOS SOI technology, *2010 Proceedings of ESSCIRC*, Seville, pp. 486–489 (2010).
22. W. Knap, D. B. But, N. Dyakonova, D. Coquillat, F. Tepe, J. Suszek, A. M. Siemion, M. Sypek, K. Szkudlarek, G. Cywinski, and I. Yahnuk, Terahertz imaging with GaAs and GaN plasma field effect transistors detectors, *2016 MIXDES - 23rd International Conference Mixed Design of Integrated Circuits and Systems*, Lodz, pp. 74–77 (2016).
23. V. M. Muravev and I. V. Kukushkin, Plasmonic detector/spectrometer of subterahertz radiation based on two-dimensional electron system with embedded defect, *Appl. Phys. Lett.*, vol. 100, p. 082102 (2012).
24. V. M. Muravev, V. V. Solov'ev, A. A. Fortunatov, G. E. Tsydynzhapov, and I. V. Kukushkin, On the response time of plasmonic terahertz detectors, *Journal of Experimental and Theoretical Physics Letters*, vol. 103, issue 12, pp. 792–794 (2012).